https://doi.org/10.22226/2410-3535-2022-4-276-281

Effect of annealing on the structure and phase composition of Cu-Al composite produced by conventional and accumulative HPT

V. N. Danilenko[†,1], L. U. Kiekkuzhina[1], N. Y. Parkhimovich[1], D. V. Gunderov[2]

[†]vdan@anrb.ru

[1]Institute for Metals Superplasticity Problems, RAS, Ufa, 450001, Russia
[2]Institute of Molecule and Crystal Physics, Ufa Federal Research Center RAS, Ufa, 450054, Russia

The paper presents the first results of the investigation of the effect of annealing on the evolution of microstructure and phase composition of a Cu-Al composite obtained by accumulative high pressure torsion (HPT). Cu-Al composites produced under 6 GPa in 10 revolutions at room temperature with conventional and accumulative HPT were annealed at 450°C for 15 min. Electron microscopy and energy dispersive spectrometry analysis showed that annealing enhances the solid-state reaction. In the sample after conventional HPT and post-deformation annealing, grayer contrast layers containing intermetallic compounds were formed at the copper-aluminum interface. The contrast on the microstructure images of the sample after accumulative HPT and post-deformation annealing is more uniform than after conventional HPT and annealing. In the sample, a more intense phase transformation occurred. This led to a noticeable increase in the volume fraction of the intermetallic compounds up to 5 – 6 times. X-ray diffraction analysis indicates that in the annealed sample after accumulative HPT, alongside with initial copper, there is also a solid solution of aluminum in copper, which differs from copper with a crystal lattice parameter. Post-deformation annealing led to the formation of different quantity of intermetallic compounds in the studied samples.

Keywords: nano-crystalline materials, accumulative HPT, phase transformations, metal matrix composite, intermetallic compounds.

1. Introduction

The structure and phase composition of polycrystalline materials play an important role in determining their physical and mechanical properties. Severe plastic deformation (SPD) is a widely used technique for changing the structure, phase composition and properties of solid state materials.

One of the most common SPD techniques is high pressure torsion (HPT). HPT after large strain degrees allows one to obtain monolithic samples that are convenient for studying the structure and measuring mechanical and physical properties [1– 3]. Recently, HPT has been further developed. For example, in [4, 5], a modified HPT technique is proposed, which allows increasing the sample size. The modified HPT proposed in [6] makes it possible to produce large shear strains in a single pass, which can be used to create hybrid materials with a gradient structure. The techniques mentioned above require significant modifications of the HPT equipment. In [7], modifications of the HPT technique is described, which is called high pressure double torsion (HPDT). In this technique, both top and bottom anvils rotate in opposite directions: clockwise and counter-clockwise, respectively. HPDT is proposed to reduce the inhomogeneity in strain distribution that occurs after conventional HPT treatment. However, the experimental results showed that the structure gradient is the same as in conventional HPT.

In [8], accumulative HPT was proposed, which is a technique that makes it possible to significantly increase the total strain and does not require modifications of the HPT equipment. The principle of the technique is in addition of a new operation to the conventional HPT. The sample, deformed in one or two revolutions, is cut into four parts, which are stacked on top of each other and deformed again. The method allowed one to achieve higher strain degrees, which go beyond the limitations of the conventional HPT [8 –10].

Conventional HPT was successfully applied to obtain composites with a metal matrix in various binary systems: Al-Cu [11–15], Cu-Al [10,11,16,17], Al-Mg [18 – 20]. Al-Nb [21, 22], Zn-Mg [23], Zr-Nb [24]. To obtain composites with a metal matrix, a stack of dissimilar plates is deformed with HPT. During deformation, the plates in the stack are being joined due to a solid-state reaction at room temperature. In some binary systems, intermetallic phases are formed during HPT deformation. Note that intermetallic compounds are formed during joining of dissimilar materials by the ARB [25] and FSW [26] methods. Annealing of the deformed samples enhances the phase formation [11,13,15 –17,19 – 23], and affects the properties of the resulting metal matrix composites [15,17,19 – 23]. Annealing of the sample of the Al-Mg binary system after HPT deformation at 300°C for 60 min resulted in a decrease in its microhardness [19]. A decrease in microhardness was also observed in the Al-Nb system upon annealing at 500°C for 30 min. Additional annealing of this sample at 550°C for 30 min showed a sharp increase in microhardness [21]. In the Cu-Al system, the samples were annealed at 450°C for 30 min. [15,16]. The main disadvantage of the obtained samples is inhomogeneous mixing along the radius of the sample. The edges of the sample are well mixed during the deformation, while the middle of the radius

and especially the center of the sample are weakly mixed. Accumulative HPT eliminates this drawback and leads to almost homogeneous mixing of the entire sample. In [10], metal-matrix composites of the Cu-Al binary system were successfully synthesized using accumulative HPT in three-layer Cu-Al-Cu stacks. Observations using scanning electron microscopy (SEM) revealed significant mixing of the Cu and Al layers and the formation of a thin lamellar structure throughout the sample volume after accumulative HPT. Accumulative HPT contributes to the solid-phase reaction and the formation of intermetallic phases $CuAl_2$ and Cu_9Al_4. In samples deformed by conventional HPT, intermetallic phases precipitate due to annealing, especially at the edges of the sample. This leads to the formation of a metal matrix composite with a heterogeneous structure along the radius. Since accumulative HPT leads to more homogeneous mixing during deformation, this technique is promising for obtaining metal matrix composites with a homogeneous structure as a result of annealing. In this regard, the purpose of this work is to study the effect of annealing on the microstructure and phase composition of the Cu-Al composite obtained by accumulative HPT.

2. Materials and experimental methods

Commercially pure copper (99.5 wt.%) and aluminum (99.1 wt.%) with a coarse-grained structure were used in the experiment. Disks with a diameter of 20.0 mm and a thickness of 0.5 mm were stacked in the order of Cu-Al-Cu, then deformed by conventional and accumulative HPT. Conventional and accumulative HPT were conducted under a pressure of 6 GPa at room temperature and with rotation speed of 1 rpm at 10 revolutions. The samples were deformed under constrained conditions with using an anvil with a depression with a diameter of 20 mm and a total depth of 0.4 mm [1]. A detailed description of the deformation conditions is given in [10].

The deformed samples were annealed in a Nabertherm HT04/17 furnace at 450°C for 15 min. The samples were loaded into a hot furnace. After annealing, the samples were removed from the hot furnace and cooled down in air to room temperature.

The macroscopic homogeneity of the annealed samples was studied in their cross sections. To prepare cross sections for study, the surface of the samples was treated with abrasive paper. Polishing was performed using a colloidal suspension based on silicon oxide. The cross sections of the annealed samples were studied using a Tescan Mira 3LMH scanning electron microscope with backscattered electron (BSE) imaging at an accelerating voltage of 20 kV. The chemical composition of the samples was studied using a Tescan VEGA 3 SBH scanning electron microscope with an energy dispersive spectroscopy (EDS) detector.

X-ray diffraction (XRD) analysis was carried out with a Bruker D8 ADVANCE diffractometer using the Bragg-Brentano scheme. The diffraction patterns were recorded in the continuous scanning mode with a speed of 0.5 deg/min within the angles 2θ from 10° to 150° using Cu radiation generated at a voltage of 40 kV and a current of 40 mA. X-ray photons were recorded using a LYNXEYE multichannel detector.

Qualitative phase analysis was performed using the PDF-2 X-ray database in the EVA software package. Quantitative phase analysis was performed using the Rietveld method in the TOPAS v. 4.2 software package. For the reliability of the analysis, the shape of the peak profiles was taken into account in accordance with their asymmetry, displacement by the angle 2θ and azimuthal tilt in relation to the incident beam. The XRD patterns were corrected using an optimized emission profile of LaB_6 obtained under the same conditions.

3. Experimental results

Microstructural and compositional maps of the annealed samples after conventional and accumulative HPT are shown in Fig. 1 and 2, respectively. In Fig. 1, in the image acquired in the BSE mode, the copper (bright) and aluminum (dark) rich areas are observed. In the central region of the sample annealed after conventional HPT, a stack of three layers is observed: copper, aluminum and copper.

Delamination occurs between the copper and aluminum layers, the cause of which was discussed in [10]. In this case, mixing of aluminum and copper did not occur. Individual inclusions of aluminum in copper and copper in aluminum are observed only on compositional maps. EDS also did not show mixing in the center of the sample.

In contrast to the central region, noticeable mixing occurred in the mid-radius of the sample. Compositional maps in Fig. 1b show that copper areas were formed in the aluminum layers, and a part of aluminum came out at the surface. At a higher magnification, this region is shown in Fig. 3 a. The layers of copper and aluminum became curved. Areas with gray contrast were formed at the boundaries of aluminum and copper.

The EDS results for the point spectra given in Table 1 and in Fig. 3 show that in the mid-radius region there are points where the ratio of aluminum and copper atoms correspond to the following intermetallic compounds: CuAl, $AlCu_3$ and $CuAl_2$.

Figure 1c shows the edge of the sample where the most noticeable structural changes occurred as a result of post-deformation annealing. In this region, a structure is observed where copper and aluminum are mixed, and the gray area has expanded. Compositional maps show the presence of a mixture of copper and aluminum. The EDS spectra analysis showed that the chemical composition corresponding to point spectra presented in Fig. 4 a and Table 2 fit to solid solutions of aluminum in copper and copper in aluminum, as well as to intermetallic compounds Al_2Cu, Al_4Cu_9, Al_9Cu_{11}.

Fig. 2 shows the microstructural and compositional maps of the annealed sample, obtained by accumulative HPT. In the central region of the sample (Fig. 2 a), we observe a well-mixed microstructure, which differs significantly from the three-layer microstructure of the annealed sample obtained by conventional HPT (Fig. 1a). A long delamination is observed and gray areas are mostly common for this case. On compositional maps, aluminum and copper formed a layered structure. EDS showed the presence of points with a chemical composition corresponding to solid solution of aluminum in copper, as well as to the intermetallic phases AlCu, Al_4Cu_9, Al_9Cu_{11}.

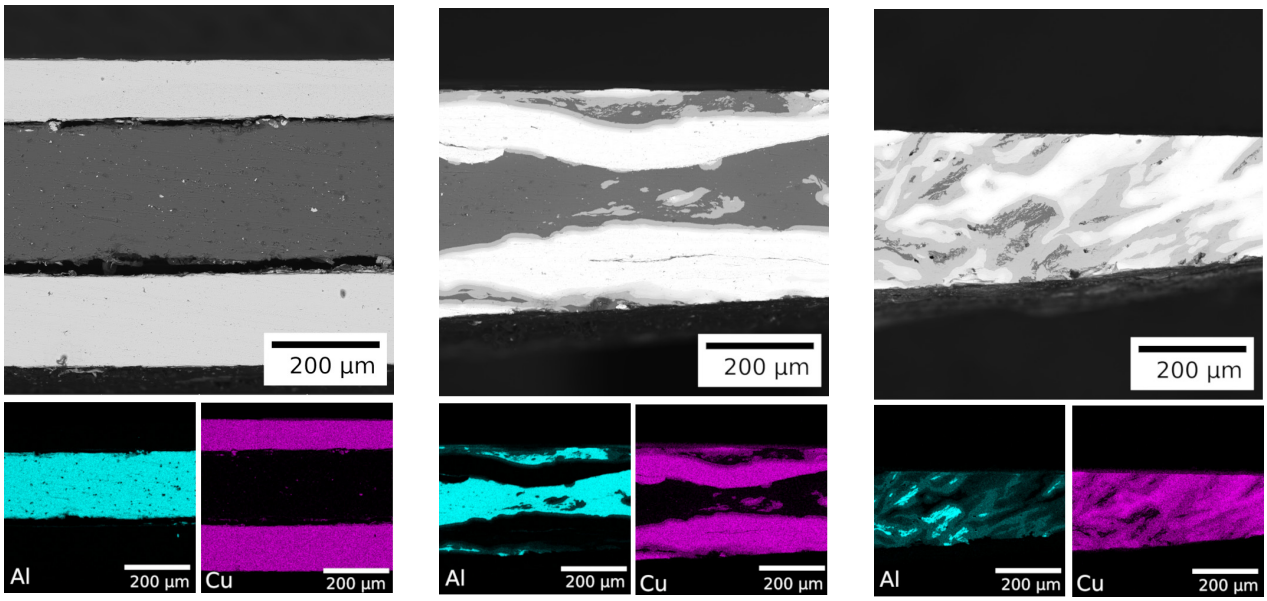

a b c

Fig. 1. (Color online) SEM BSE cross-sectional images and corresponding compositional maps of Al and Cu of the sample after conventional HPT and annealing in the region of the center (a), mid-radius (b) and edge (c).

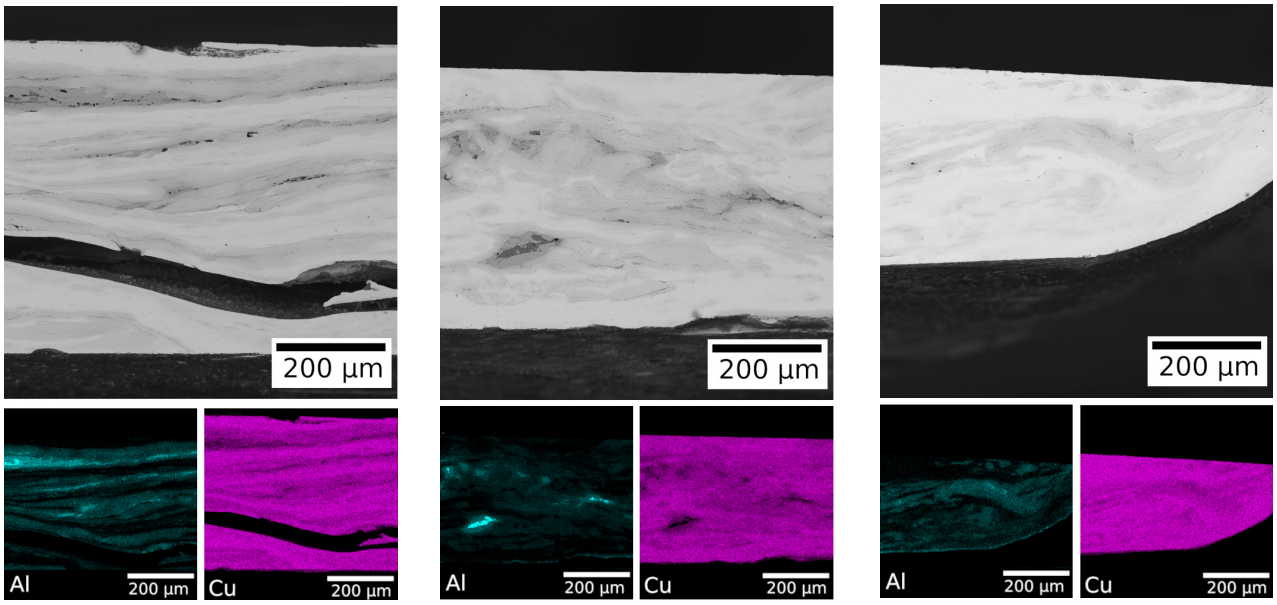

a b c

Fig 2. (Color online) SEM BSE cross-sectional images and corresponding composition maps of Al and Cu of the sample after accumulative HPT and annealing in the region of the center (a), mid-radius (b) and edge (c).

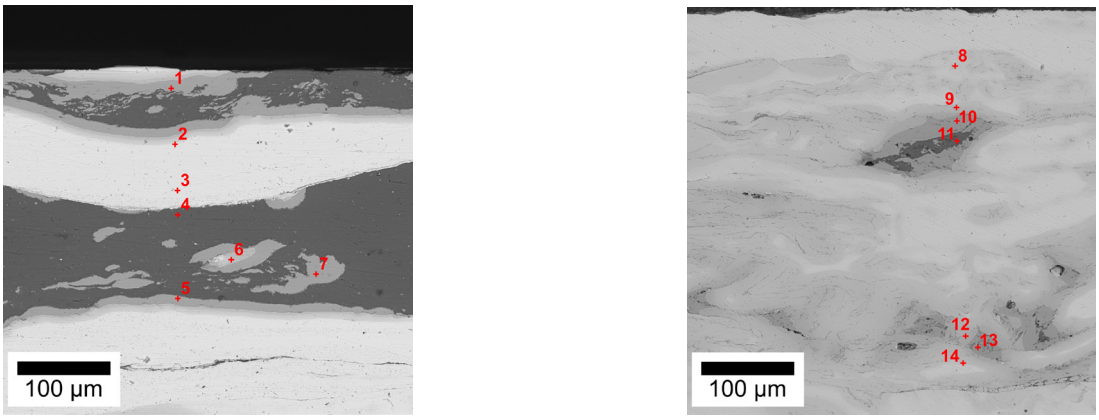

a b

Fig. 3. SEM BSE cross-sectional images with points of EDS spectra acquisition of the annealed samples after conventional (a) and accumulative (b) HPT in the region of mid-radius.

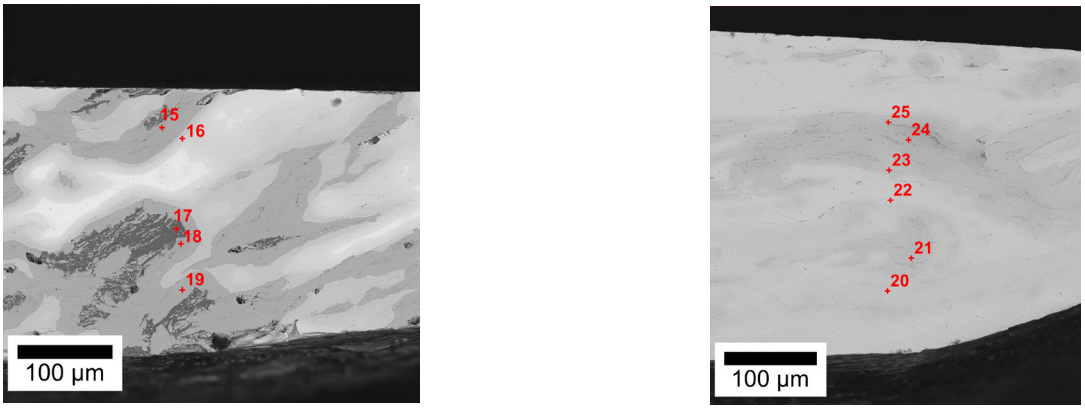

a b

Fig. 4. SEM BSE cross-sectional images with points of EDS spectra acquisition of the annealed samples after conventional (a) and accumulative (b) HPT in the region of edge.

Noticeable mixing is also observed in the mid-radius of the sample (Fig. 2b). On the compositional maps in Fig. 2b, it can be seen that the aluminum fraction has noticeably decreased. The EDS results shown in Table 1 and in Fig. 3b indicate the presence of intermetallic phases CuAl, Al_4Cu_9, Al_9Cu_{11}, $AlCu_3$, and $CuAl_2$ and a solid solution of copper in aluminum (point 11 in Fig. 3b).

The weaker contrast in the BSE images indicates that at the the structure is significantly mixed at edge of the sample. On the compositional maps, most of the area corresponds to copper, and a small amount of aluminum remains. EDS (Fig. 4b and Table 2) showed the presence of points with a chemical composition corresponding to the intermetallic phases CuAl, Al_4Cu_9, $AlCu_3$ and a number of points corresponding to a solid solution of aluminum in copper.

XRD analysis revealed that post-deformation annealing led to changes in the phase composition of the samples. According to the XRD pattern showed in Fig. 5a, in the sample obtained by annealing after conventional HPT there are peaks of copper, aluminum, and a peak of the Al_4Cu_9 intermetallic compound from the (114) plane. Phase composition of the sample annealed after conventional HPT. shown in Table 3.

The XRD pattern of the sample obtained with annealing after accumulative HPT showed that the aluminum peak has a minimum intensity (Fig. 5b). The diffraction peak from the (112) plane of Al_2Cu and the (114) plane of Al_4Cu_9 and the intensity of the copper peak decreased noticeably in relation to the peaks of the intermetallic phases. The Rietveld analysis showed the presence of intermetallic phases, copper, and a solid solution of aluminum in copper. Copper and a solid solution of aluminum in copper have different crystal lattice parameters. The crystal lattice parameter of copper is $a = 0.36222(5)$ nm, and the crystal lattice parameter of the solid solution of aluminum in copper, designated in Table 3 as Cu (Al), is $a = 0.36534(5)$ nm. The phase composition of the sample annealed after accumulative HPT is shown in Table 3.

4. Discussion

As shown in [10], accumulative HPT leads to mixing of copper and aluminum in the entire volume of a deformed three-layer Cu-Al-Cu sample. Conventional HPT allows

Table 1. EDS results for the points shown in Fig. 3.

Points	Elemental composition		Possible IMCs
	Al, at.%	Cu, at.%	
1	66.5	33.5	Al_2Cu
2	5.1	94.9	$AlCu_3$
3	0.3	99.7	Cu
4	98.4	1.6	Al(Cu)
5	67.3	32.7	Al_2Cu
6	46.9	53.1	AlCu
7	66.8	33.2	Al_2Cu
8	22.9	77.1	$AlCu_3$
9	33.6	66.4	Al_4Cu_9
10	65.4	34.6	Al_2Cu
11	97.7	2.3	Al(Cu)
12	45.7	54.3	Al_2Cu
13	65.3	34.7	Al_9Cu_{11}
14	27.7	72.3	$AlCu_3$

Table 2. EDS results for the points shown in Fig. 4.

Points	Elemental composition		Possible IMCs
	Al, at.%	Cu, at.%	
15	64.7	35.3	Al_2Cu
16	38.7	61.3	Al_2Cu_3
17	95.8	4.2	Al(Cu)
18	66.1	33.9	Al_2Cu
19	66.5	33.5	Al_2Cu
20	15.7	84.3	Cu(Al)
21	30.6	69.4	Al_4Cu_9
22	2.6	97.4	Cu(Al)
23	27.7	72.3	$AlCu_3$
24	39.7	60.3	Al_2Cu_3
25	33.5	66.5	Al_4Cu_9

Table 3. Phase composition of the samples obtained by XRD (HPT — conventional, ACC HPT — accumulative).

Phase	HPT, %	ACC HPT, %
Al	24.0	1.3
Cu	67.7	25.9
Cu(Al)	-	27.3
Al_2Cu	2.1	2.7
Al_4Cu_9	5.4	35.2
AlCu	0.8	7.6

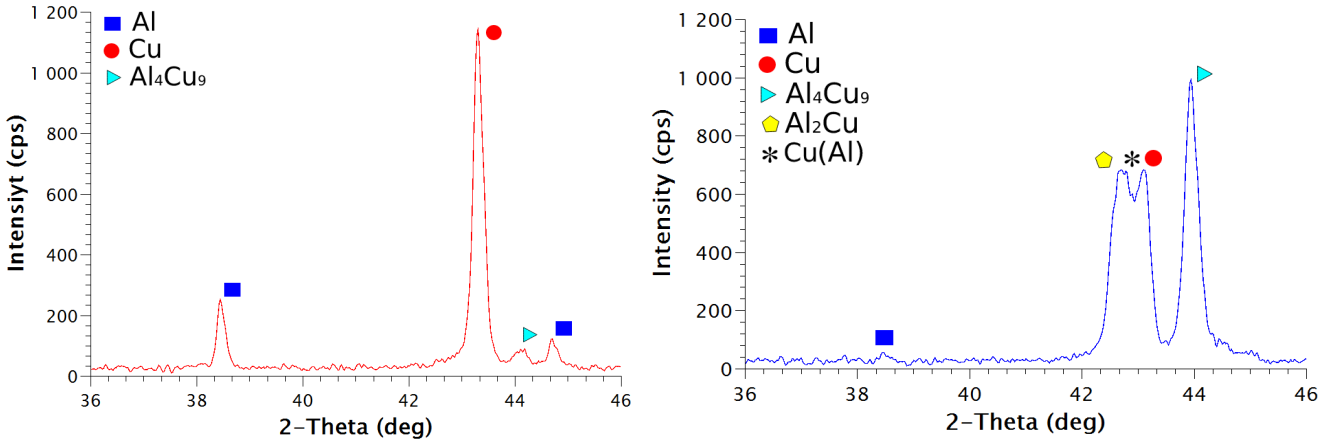

Fig. 5. (Color online) XRD patterns of annealed Cu-Al-Cu samples after conventional (a) and accumulative HPT (b).

only the edge of the sample to be well mixed, as a result of inhomogeneous deformation along the radius.

As can be seen from Figs. 1 and 2, annealing at 450°C for 15 min led to different contrast in BSE images of the structure of the studied samples. A significant feature of the structure in the provided images is the presence of gray areas at the interface of the copper and aluminum layers in conventional HPT whereas in case of accumulative HPT most of the cross section of the sample consists of grey areas. These features in the BSE image of the annealed samples indicate the presence of diffusion resulted in changes in the phase composition of the samples. The results of the point spectra EDS analysis shown in Fig. 3 and 4, as well as in Tables 1 and 2, confirm that areas with different grey contrast in the BSE image correspond to different intermetallic phases.

In the literature, phase transformations during the formation of metal matrix composites are associated with diffusion [12,17–19,21,22]. The role of diffusion was described in detail in [27]. It was shown that the lattice diffusion coefficient becomes comparable with the surface diffusion coefficient. A large number of defects induced during HPT enhances diffusion.

The XRD method showed a difference in the phase composition of the annealed samples. In the sample annealed after conventional HPT, we observe the presence of three main phases: Al, Cu, and Al_4Cu_9, as well as a small amount of Al_2Cu and AlCu phases. The phase composition in the annealed sample after accumulative HPT changes significantly: a noticeable growth of intermetallic phases takes place. The fraction of intermetallic phases in the sample subjected to annealing after accumulative HPT is several times larger than that in the sample annealed after conventional HPT (Table 3). The dissolution of aluminum during annealing probably led to the formation of intermetallic compounds and solid solution of aluminum in copper Cu(Al). The formation of Cu(Al) phase may be related to the high (up to 18 at.% [28]) solubility of aluminum in copper and homogeneous mixing of the initial components during accumulative HPT which requires further study. Comparison of the phase composition of the studied samples indicates that the accumulative HPT technique is useful for forming the intermetallic phases during annealing. As it was shown in [10], accumulative HPT led to homogeneous mixing in entire volume of the sample in contrast to conventional HPT. One can presume that alongside with diffusion, homogeneous mixing in the entire volume of the sample obtained by accumulative HPT is the reason for such a significant difference in phase formation in the studied samples.

5. Summary and conclusions

Scanning electron microscopy and energy dispersive spectroscopy have shown that annealing the sample obtained by accumulative HPT leads to a more homogeneous distribution of phases over the entire volume of the sample than annealing of a sample obtained by conventional HPT.

X-ray phase analysis showed that in the annealed sample after accumulative HPT, along with copper ($a = 0.36222(5)$ nm), a phase of a solid solution of aluminum in copper ($a = 0.36534(5)$ nm) was detected.

The proportion of intermetallic phases as a result of annealing the sample obtained by accumulative HPT increased by several times in comparison with the annealed sample after conventional HPT. The annealed sample after conventional HPT contains the following intermetallic compounds: Al_4Cu_9 (5.4%), Al_2Cu (2.1%), AlCu (0.8%). The following intermetallic compounds were found in the annealed sample after accumulative HPT: Al_4Cu_9 (35.2%), AlCu (7.6%), Al_2Cu (2.7%).

Acknowledgements. The work was supported by the RSF grant № 22-19-00347 and partially supported by the state assignment of the IMSP RAS № 122011900426-4. Electron microscopy studies were carried out on the facilities of the shared services center of IMSP RAS "Structural and Physical-Mechanical Studies of Materials". XRD studies were carried out on the facilities of regional shared services center of UFRC RAS "Agidel".

References

1. A.P. Zhilyaev, T.G. Langdon. Progr. Mater. Sci. 53, 893 (2008). Crossref

2. A.P. Zhilyaev, A.I. Pshenichnyuk, F.Z. Utyashev, G.I. Raab. Superplasticity and grain boundaries in ultrafine-grained materials. Woodhead Publishing (2021) 416 p.
3. H. Azzeddine, D. Bradai, T. Baudin, T.G. Langdon. Prog. in Mater. Sci. 125, 100866 (2022). Crossref
4. K. Edalati, Z. Horita. J. Mater. Sci. 45, 4578 (2010). Crossref
5. A. Hohenwarter. Mater. Sci. Eng. A. 626, 80 (2015). Crossref
6. Yu. Ivanisenko, R. Kulagin, V. Fedorov, A. Mazilkin, T. Scherer, B. Baretzky, H. Hahn. Mater. Sci. Eng. A. 664, 247 (2016). Crossref
7. M. Jahedi, M.H. Paydar, Sh. Zheng, I.J. Beyerlein, M. Knezevic. Materials Science & Engineering A. 611, 29 (2014). Crossref
8. D.V. Gunderov, A.A. Churakova, V.V. Astanin, R.N. Asfandiyarov, H. Hahn, R.Z. Valiev. Mater. Lett. 261, 127000 (2020). Crossref
9. D. Gunderov, A. Stotskiy, Y. Lebedev, V. Mukaeva. Metals. 11, 573 (2021). Crossref
10. V.N. Danilenko, L.U. Kiekkuzhina, N.Y. Parkhimovich, E.D. Khafisova, D.V. Gunderov. Materials Letters. 300, 130240 (2021). Crossref
11. V.N. Danilenko, G.F. Korznikova, A.P. Zhilyaev, S.N. Sergeev, G.R. Khalikova, R.K. Khisamov, K.S. Nazarov, L.U. Kiekkuzhina, R.R. Mulyukov. IOP Conf. Ser. Mater. Sci. Eng. 447, 012021 (2018). Crossref
12. J.-K. Han, D.K. Han, G.Y. Liang, J.-I. Jang, T.G. Langdon, M. Kawasaki. Adv. Eng. Mater. 20, 1800642 (2018). Crossref
13. G.F. Korznikova, K.S. Nazarov, R.K. Khisamov, S.N. Sergeev, R.U. Shayachmetov, G.R. Khalikova, J.A. Baimova, A.M. Glezer, R.R. Mulyukov. Materials Letters. 253, 412 (2019). Crossref
14. P. Bazarnik, A. Bartkowska, B. Romelczyk-Baishya, B. Adamczyk-Cieslak, J. Dai, Y. Huang, M. Lewandowska, T.G. Langdon. Journal of Alloys and Compounds. 846, 156380 (2020). Crossref
15. G. Korznikova, R. Kabirov, K. Nazarov, R. Khisamov, R. Shayakhmetov, E. Korznikova, G. Khalikova, R. Mulyukov. JOM. 72, 2898 (2020). Crossref
16. V.N. Danilenko, R.M. Mazitov. Nanotechnology and Science of Nanocrystalline Materials. Collection of seminar topics. Ekaterinburg, Russia (2005) p. 280. (in Russian)
17. V.N. Danilenko, S.N. Sergeev, J.A. Baimova, G.F. Korznikova, K.S. Nazarov, R.K. Khisamov, A.M. Glezer, R.R. Mulyukov. Materials Letters. 236, 51 (2019). Crossref
18. B. Ahn, A.P. Zhilyaev, H.-J. Lee, M. Kawasaki, T.G. Langdon. Mater. Sci. and Eng. A. 635, 109 (2015). Crossref
19. J.-K. Han, H.-J. Lee, M. Kawasaki, T.G. Langdon. Mater. Sci. and Eng. A. 684, 318 (2017). Crossref
20. M. Kawasaki, J.-K. Han, D.-H. Lee, J.-I. Jang, T.G. Langdon. J. Mater. Res. 33, 2700 (2018). Crossref
21. V.N. Danilenko, S.N. Galishev, R.R. Mulyukov. Perspective Materials. 7, 94 (2009). (in Russian)
22. G. Korznikova, E. Korznikova, K. Nazarov, R. Shayakhmetov, R. Khisamov, G. Khalikova, R. Mulyukov. Adv. Eng. Mater. 23, 2000757 (2020). Crossref
23. D. Hernández-Escobar, J. Marcus, J.K. Han, R.R. Unocic, M. Kawasaki, C.J. Boehlert. Mater. Sci. and Eng. A. 771, 138578 (2020). Crossref
24. D. Luo, T. Huminiuc, Y. Huang, T. Polcar, T.G. Langdon. Mater. Sci. and Eng. A. 790, 139693 (2020). Crossref
25. V.Y. Mehr, M.R. Toroghinejad, A. Rezaeian. Materials Science & Engineering A. 601, 40 (2014). Crossref
26. V.N. Danilenko, L.U. Kiekkuzhina, A.S. Selivanov, Yu.V. Logachov, V.V. Atroshenko, R.R. Mulyukov. Letters on Materials. 12 (2), 106 (2022). Crossref
27. K. Oh-Ishi, K. Edalati, H.S. Kim, K. Hono, Z. Horita. Acta Mater. 61, 3482 (2013). Crossref
28. X.J. Liu, I. Ohnuma, R. Kainuma, K. Ishida. J. Alloys Compd. 264, 201 (1998). Crossref